BECC-engineered live-attenuated *Shigella* vaccine candidates display reduced endotoxicity with robust immunogenicity in mice

Matthew E. Sherman [a], Jane Michalski [a,b], Sayan Das [a], Hyojik Yang [a], Lakshmi Chandrasekaran [c], Timothy R. O'Meara [d], David J. Dowling [d,e], Ofer Levy [d,e,f], Shoshana Barnoy [c], Malabi Venkatesan [c], Robert K. Ernst [a,*]

[a] *University of Maryland-Baltimore, Department of Microbial Pathogenesis, Baltimore, MD 21201, USA*
[b] *University of Maryland School of Medicine, Institute for Genome Sciences, Baltimore, MD 21201, USA*
[c] *Walter Reed Army Institute of Research, Department of Diarrheal Disease Research, Bacterial Disease Branch, Silver Spring, MD 20910, USA*
[d] *Precision Vaccines Program, Department of Pediatrics, Boston Children's Hospital, Boston, MA 02115, USA*
[e] *Harvard Medical School, Boston, MA 02115, USA*
[f] *Broad Institute of MIT & Harvard, Cambridge, MA 02142, USA*

ARTICLE INFO

ABSTRACT

Shigella spp. infection contributes significantly to the global disease burden, primarily affecting young children in developing countries. Currently, there are no FDA-approved vaccines against *Shigella,* and the prevalence of antibiotic resistance is increasing, making therapeutic options limited. Live-attenuated vaccine strains WRSs2 (*S. sonnei*) and WRSf2G12 (*S. flexneri* 2a) are highly immunogenic, making them promising vaccine candidates, but possess an inflammatory lipid A structure on their lipopolysaccharide (LPS; also known as endotoxin). Here, we utilized bacterial enzymatic combinatorial chemistry (BECC) to ectopically express lipid A modifying enzymes in WRSs2 and WRSf2G12, as well as their respective wild-type strains, generating targeted lipid A modifications across the *Shigella* backgrounds. Dephosphorylation of lipid A, rather than deacylation, reduced LPS-induced TLR4 signaling *in vitro* and dampened endotoxic effects *in vivo*. These BECC-modified vaccine strains retained the phenotypic traits of their parental strains, such as invasion of epithelial cells and immunogenicity in mice without adverse endotoxicity. Overall, our observations suggest that BECC-engineered live attenuated vaccines are a promising approach to safe and effective *Shigella* vaccines.

1. Introduction

Shigella are Gram-negative bacteria known to cause diarrheal disease in humans through ingestion of contaminated food and water [1–4]. Of the four pathogenic *Shigella* species (*S. sonnei*, *S. flexneri*, *S. boydii*, and *S. dysenteriae*), *S. sonnei* (*Ss*) and *S. flexneri* (*Sf*) cause the majority of disease in industrialized and developing countries, respectively [5]. Shigellosis (*Shigella*-induced diarrhea) affects all age groups but particularly plagues young children as uncontrolled inflammation and severe dehydration can lead to growth abnormalities, seizure, and even death [2,6–9]. The clinical severity [10,11] and emergence of antibiotic resistance [12,13] have prompted the development of multiple *Shigella* vaccine candidates that are currently in preclinical and clinical phases [4,14]. However, to date, there is no FDA-licensed *Shigella* vaccine.

Protection against shigellosis is serotype-specific [4,5,14,15], implicating the O-antigen component of lipopolysaccharide (LPS) as being the critical antigen for vaccine development. Vaccine strategies to prevent shigellosis have included glycoconjugate vaccines where the O-antigen is conjugated to carrier adjuvants [4,5,14–16], an oligomeric complex comprised of LPS and the invasion plasmid antigens (Ipa) called Invaplex [17–19], and outer-membrane vesicles (OMVs) produced *via* the generalized modules for membrane antigens (GMMA) method [20–23]. Another longstanding strategy has been the development of live-attenuated *Shigella* strains where the O-antigen remains in its native context on the outer membrane [4,5,14,15,24]. Current live-attenuated vaccine candidates focus primarily on *S. sonnei* and *S. flexneri* serotype 2a*,* which are epidemiologically significant *Shigella* strains [25] and whose O-antigen structures are well characterized [15].

A key advantage of live-attenuated *Shigella* vaccines, which generally contain genetic mutations or deletions in virulence-associated genes

[5,14], is that they mimic a natural *Shigella* infection and, therefore, generate an immune response that protects against future infection. While these vaccines induce protective immune responses against virulent challenge in volunteer studies [26], significant issues including adverse reactogenicity have slowed the progress toward a universally accepted safe and effective *Shigella* vaccine [4,5,14]. For this study, we used the live-attenuated vaccine candidates WRSs2 (*S. sonnei* strain) and WRSf2G12 (*S. flexneri* 2a strain), developed by Walter Reed Army Institute of Research (WRAIR), which are principally attenuated by deletion of *virG* (also known as *icsA*) thereby prohibiting intercellular spread but also contain deletions in genes encoding enterotoxins [27–35]. WRSs2 and WRSf2G12 are second-generation vaccines whose first-generation counterparts (WRSS1 and SC602, respectively) were highly immunogenic in adults and children during clinical trials, but substantial reactogenicity was observed at the moderate to high doses required to confer protective immunity [26,36–41]. In a phase I clinical trial, WRSs2 was generally well tolerated but still not at a satisfactory level where it can be used as a safe vaccine [42]. To improve the safety of WRSs2 and WRSf2G12 we chose to target the highly immunostimulatory LPS molecule present on the bacterial membrane, which is thought to be a major contributor to these adverse effects.

LPS is a glycolipid present on the outer membrane of Gram-negative bacteria and is composed of three regions: the O-antigen, core oligosaccharide, and lipid A membrane anchor [43,44]. Innate immune cells can recognize the lipid A region of LPS and initiate cytokine production to alert the immune system to the presence of a bacterial invader [45]. This occurs through a series of accessory proteins that guide the binding of lipid A to the TLR4/MD-2 receptor on the surface of innate immune cells to drive downstream signaling, such as the NF-κB pathway, and induce pro-inflammatory cytokine production [46,47]. The TLR4/MD-2 response is primarily driven by the structural features of lipid A, which vary across Gram-negative bacteria [45,46,48,49]. *Shigella* synthesizes a prototypical lipid A structure comprised of six acyl chains (hexa-acylated) and two terminal phosphates (bis-phosphorylated) [45]. This structure is a potent stimulator of TLR4/MD-2 [21], and the ensuing pro-inflammatory cytokine production likely contributes to the febrile symptoms observed upon oral ingestion of *Shigella* for vaccination. Thus, the immunostimulatory lipid A moiety was the primary target for detoxification.

In this study, we employed bacterial enzymatic combinatorial chemistry (BECC) [50] to detoxify WRSs2 and WRSf2G12, as well as their respective wild-type strains. Lipid A modifying enzymes LpxE (1-position phosphatase from *Francisella*) and PagL (3-position deacylase from *Salmonella*) were ectopically expressed in the *Shigella* backgrounds. Targeted lipid A dephosphorylation (LpxE), deacylation (PagL), or execution of both modifications (Dual) was confirmed using MALDI-TOF MS. Lipid A dephosphorylation, rather than deacylation, effectively diminished LPS-induced pro-inflammatory immune signaling. Furthermore, deacylation combined with dephosphorylation did not further reduce LPS-mediated signaling. Due to this, only dephosphorylated lipid A mutants (LpxE-modified) were generated in WRSs2 and WRSf2G12, generating WRSs2E and WRSf2G12E. These strains had reduced LPS-mediated pro-inflammatory cytokine production *in vitro* and severely blunted endotoxemia *in vivo,* yet they remained as capable as their parental strains to invade epithelia and generate immunogenicity against their O-antigen. Altogether, we characterize two live-attenuated *Shigella* vaccine candidates (WRSs2E and WRSf2G12E), altered only in their lipid A region, which are greatly detoxified without any consequence to phenotypic traits suggesting that such live-attenuated strains are a promising approach to develop a safe and effective *Shigella* vaccine.

2. Results

2.1. Targeted lipid A modifications in Shigella

We initially utilized our BECC system to engineer targeted lipid A

modifications (Fig. 1) in *S. sonnei* Moseley and *S. flexneri* 2a 2457T, the wild-type (WT) strains upon which WRSs2 and WRSf2G12 were derived, respectively. Expression of the lipid A biosynthetic enzymes LpxE and PagL alone, or in combination (termed "Dual"), from the osmotically inducible pSEC10 plasmid resulted in targeted modification of the lipid A structure, which was confirmed *via* MALDI-TOF MS analysis (Fig. S1A, B). Successful lipid A modification in WT strains prompted the expression of the individual enzymes in first-generation live-attenuated vaccine strains WRSS1 and SC602. Similar to the WT strains, upon plasmid-based expression of BECC constructs, lipid A dephosphorylation and deacylation were observed in WRSS1 and SC602 by MALDI-TOF MS (Fig. S1C, D). In all the *Shigella* backgrounds tested, PagL-modification was accompanied by spontaneous lipid A dephosphorylation (Fig. S1A—D), suggesting that plasmid-based expression of *pagL* may induce lipid A phosphatase activity *via* an unknown mechanism. Despite this, the MALDI-TOF MS data suggested that targeted lipid A modifications could be achieved in both WT and genetically attenuated strains of *Shigella*.

We next assessed whether these targeted lipid A modifications affected the immunostimulatory capacity of *Shigella* LPS. Purified LPS from Moseley and 2457T was normalized to keto-deoxy-octanoate (Kdo), a conserved sugar within the core oligosaccharide, and used to stimulate NF-κB reporter cells. For LPS from Moseley, stimulation with LpxE- and Dual-modified LPS resulted in a pronounced reduction in NF-κB signaling compared to WT LPS, whereas stimulation with PagL-modified LPS generated comparable NF-κB signaling to that of WT LPS (Fig. S2A). For LPS from 2457technicallyT, however, only the LpxE-modification reduced NF-κB signaling compared to WT LPS (Fig. S2B). This suggested that lipid A dephosphorylation, rather than deacylation, was the most promising modification for reduced endotoxicity, and therefore, only the LpxE- and Dual-modification were pursued for the remainder of the study.

To remove the need for ectopic plasmid expression of the lipid A modification enzymes, we utilized Tn7 transposition to insert the *lpxE* and Dual gene cassettes into the chromosome of Moseley and 2457T. In this approach, insertion occurs exclusively at the *attTn7* site located at the 3' end of the highly conserved *glmS* gene and is known not to disrupt any chromosomal genes or the bacterial fitness [51]. Using the same approach, second-generation vaccine strains WRSs2 and WRSf2G12 were also chromosomally integrated with *lpxE*; however, the Dual gene cassette could not be chromosomally integrated into these specific vaccine strains. For the remainder of the study, these chromosomally integrated strains were utilized. Moseley and 2457T are designated with LpxE[+] or Dual to indicate what chromosomal integration they contain. Vaccine strains WRSs2 and WRSf2G12 chromosomally integrated with *lpxE* are designated as WRSs2E and WRSf2G12E, respectively.

Using MALDI-TOF MS, we confirmed that chromosomal expression of *lpxE* and Dual resulted in lipid A modification across the various *Shigella* backgrounds (Fig. 2). Site-specificity of the lipid A modifications was confirmed *via* MALDI-TOF MS/MS using the FLAT[n] approach [52]. WT, LpxE-, and Dual-modified LPS each synthesized their expected base peaks at *m/z* 1797, 1717, and 1490, respectively (Fig. S3A), which were selected as the precursor ions for fragmentation (Fig. S3B, circled in red). The large cluster of spectral peaks at *m/z* less than 1490 represents cardiolipin (Fig. S3A), another phospholipid that resides in the outer leaflet along with lipid A. Spectral peaks representing fragments from the precursor ions (Fig. S3B) were mapped to the proposed chemical structures of WT, LpxE-, and Dual-modified *Shigella* lipid A (Fig. S3C). Determination of the location of the terminal phosphate modification at the 1-position was confirmed by the fragment ion still present at *m/z* 690 in the LpxE-modified structure, and the deacylation modification at the 3-position was confirmed by the ions generated from the $^{0,2}A_2$ cross-ring cleavage event (Fig. S3C). Furthermore, SDS-PAGE and subsequent Pro-Q Emerald 300 staining of LPS extracted from the LpxE- or Dual-modified strains showed no alterations to the O-antigen region compared to their parental counterparts, suggesting the modifications
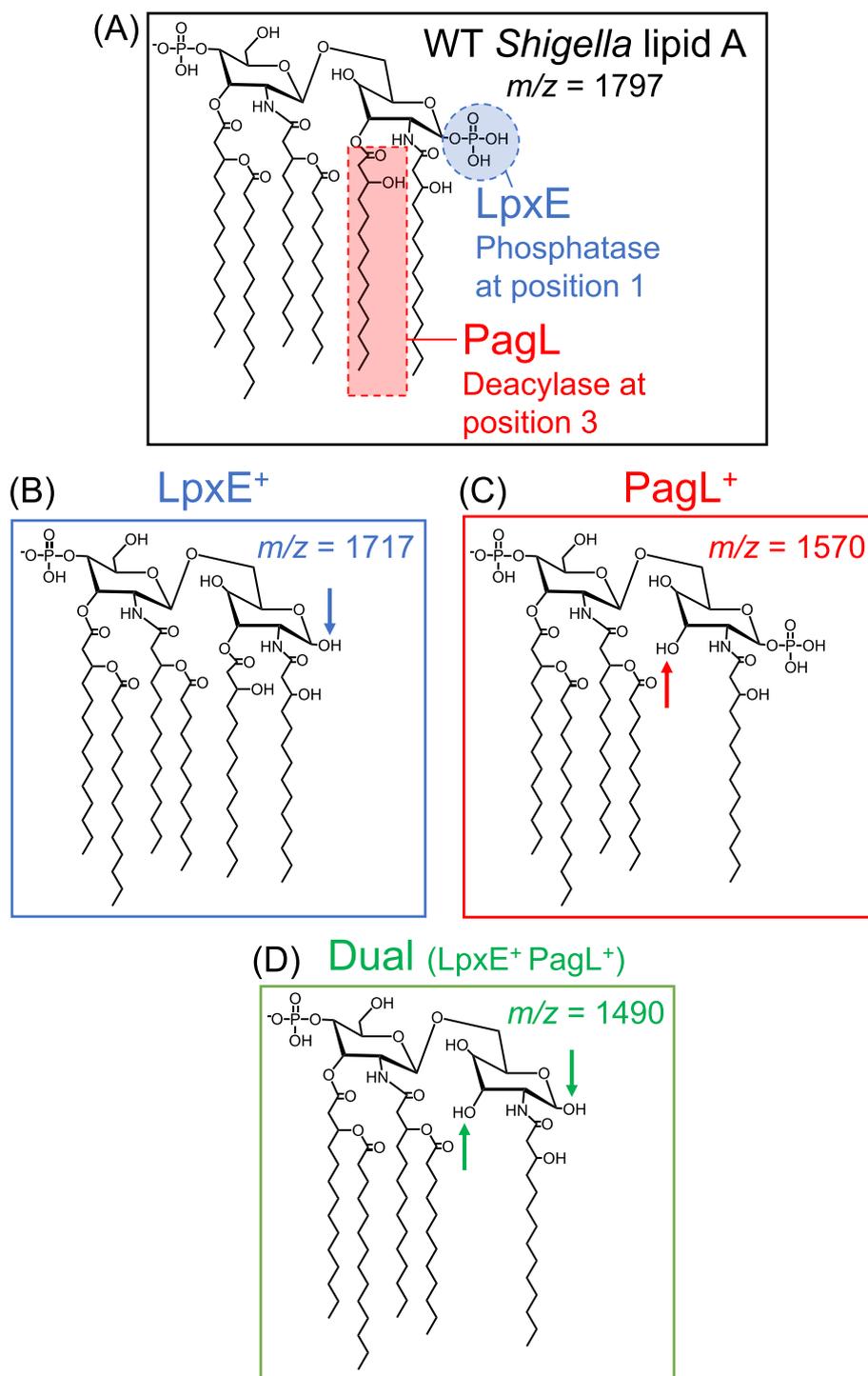
Fig. 1. Lipid A modifications generated by BECC constructs used in this study. (A) The WT lipid A structure of *Shigella* along with the (B) LpxE- (C) PagL- and (D) Dual-modified resultant structures, lacking a phosphate, 3OH C14 acyl chain, or both, respectively. The epxected *m/z* for the [M-H]⁻ ions observed in MALDI-TOF spectra are displayed for each structure.

were specific to the lipid A region (Fig. S4).

2.2. BECC-modified Shigella strains phenocopy their isogenic parental strains

Live-attenuated *Shigella* strains have fundamental requirements that enable them to function as effective oral vaccines. First, large-scale production requires efficient growth in culture. Secondly, these strains must be capable of invading gut epithelia, a step during infection that elicits the host immune response required for mucosal immunity [14]. Lastly, host defense responses must be unaltered, such as the secretion of CXCL8 from the gut epithelia, which recruits polymorphonuclear leukocytes to the site of infection to clear the bacteria [10]. Thus, any limitation with respect to growth, invasion, or the host response would render our BECC-modified *Shigella* strains unsuitable to be used as vaccine candidates.

To evaluate the capacity to grow in culture, we assayed the growth kinetics of our BECC-modified *Shigella* and compared it to their isogenic
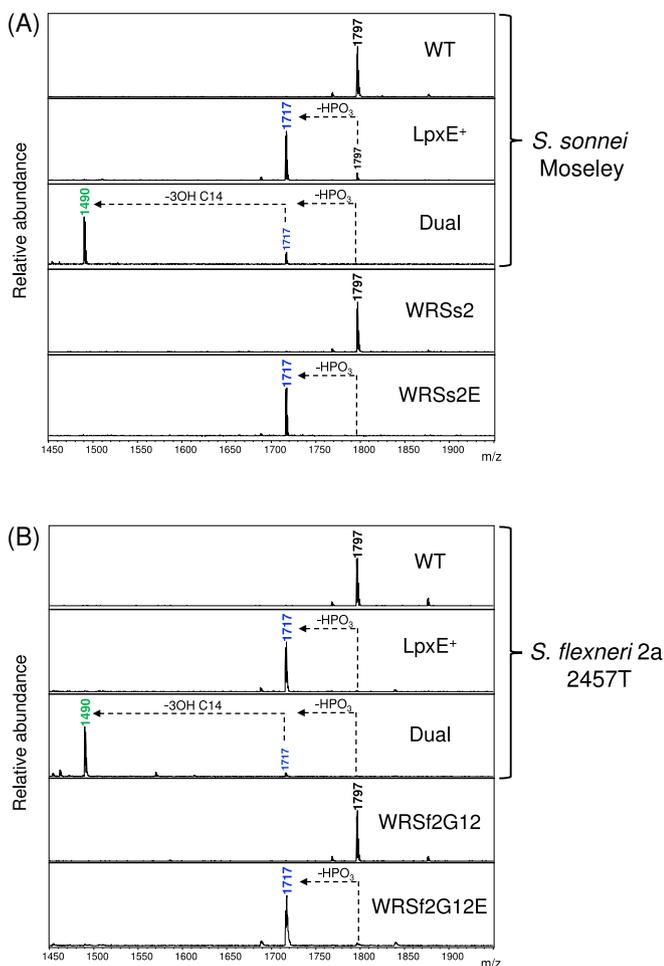
Fig. 2. MALDI-TOF MS analysis of lipid A related peaks from BECC-modified *Shigella.* Representative MALDI-TOF MS spectra for (A) *S. sonnei* and (B) *S. flexneri* 2a strains chromosomally expressing *lpxE* or Dual. Spectral peaks represent [M-H]⁻ ions. Colored peaks correspond to the expected structures detailed in Figure 1. Arrows depict the loss of a phosphate (HPO₃) or acyl chain (3OH C14) from the indicated lipid A species.

parental strains. Over the course of 15 h, BECC-modified *Shigella* showed minimal growth alterations as compared to their unmodified counterparts (Fig. S5), suggesting BECC-modification had minimal impact on the capacity of the *Shigella* strains to grow *in vitro*.

To evaluate the invasion of epithelia by *Shigella* (intracellular bacterial burden recovered as a percentage of the inoculum), we employed a gentamicin protection assay [30,32,33]. The BECC-modified *S. sonnei* strains invaded similarly to their parental strains. As found previously [30], WRSs2 strains invaded the epithelial cells significantly more than the Moseley strains (Fig. 3A). For *S. flexneri* 2a strains, while LpxE-modification did not impact invasiveness, Dual-modification resulted in a significantly lower invasion than the WT (Fig. 3B), likely due to a high frequency of invasion plasmid loss compared to the other *S. flexneri* 2a strains (data not shown). Beyond invasion, we also measured CXCL8 concentrations in the supernatant to assess the host response to infection, which showed the same pattern as invasion (Fig. 3C, D). This suggested that, except for the Dual-modification in 2457T, the targeted lipid A modifications did not impact the phenotypic traits of *Shigella,* such as growth, invasion of gut epithelia, or the host response to infection.

2.3. Lipid A modifications reduced endotoxicity in vitro and in vivo

Since detoxification of *Shigella* lipid A was the primary objective of

this study, we determined the level of endotoxicity using purified LPS from the chromosomally integrated strains. HEK-Blue cells containing an NF-κB reporter and stably expressing either the human or mouse orthologs of TLR4/MD-2/CD-14 were stimulated with Kdo normalized LPS. Stimulation with LPS from WRSs2E or WRSf2G12E displayed reduced NF-κB signaling compared to LPS from their respective parental strain (Fig. 4A, B). Similar results were observed upon stimulating HEK-Blue cells with LPS from BECC-modified 2457T and Moseley (Fig. S6A, B) or upon stimulation of macrophage NF-κB reporter cells that express endogenous levels of TLR4/MD-2/CD-14 (Fig. S7). In both cases, LpxE- and Dual-modified LPS blunted NF-κB signaling to a similar degree (Fig. S6A, B, S7), suggesting lipid A dephosphorylation alone was sufficient to reduce the LPS-mediated TLR4 signaling.

To examine the LPS-induced TLR4 signaling in primary cells, we stimulated human peripheral blood monocytes (PBMCs) with LPS and assayed the supernatant for cytokine production. Notably, production of TNF-α, IL-1β, IL-10, and IL-6 was dampened upon stimulation with LPS from WRSs2E or WRSf2G12E compared to LPS from their parental strains, albeit the reduction in WRSs2E was more modest than that observed for WRSf2G12E (Fig. 4C). Similarly, stimulation of PBMCs with LPS from 2457T had lower cytokine production for BECC-modified LPS compared to WT LPS (Fig. S6C). BECC-modified LPS from Moseley demonstrated similar cytokine levels to that of BECC-modified LPS from 2457T; however, WT LPS from Moseley was less stimulatory than expected (Fig. S6C). A separate experiment showed that LpxE- and Dual-modified LPS from Moseley displayed reduced induction of TNF-α from PBMCs, and to a similar degree, compared to WT LPS (Fig. S6D). This confirmed that dephosphorylated *Shigella* lipid A does indeed reduce pro-inflammatory responses across all the *Shigella* backgrounds.

To confirm that the BECC-modified LPS was also detoxified *in vivo*, we employed an acute murine endotoxicity study whereby a normally lethal dose of LPS was injected intraperitoneally into mice, and their health status monitored over the course of 72 h. Whereas injection of LPS from WRSf2G12 or WRSs2 was lethal by 24 h post-injection, all mice receiving the same dose of LPS from WRSf2G12E or WRSs2E survived (Fig. 4D). Similarly, mice receiving WT LPS from 2457T or Moseley succumbed to acute endotoxemia whereas mice receiving BECC-modified LPS from 2457T or Moseley survived (Fig. S6E). This, combined with the NF-κB reporter and PBMCs data, suggested that dephosphorylation of lipid A was sufficient to reduce endotoxicity both *in vitro* and *in vivo*.

2.4. LpxE-modification did not compromise the immunogenicity of the Shigella vaccine strains

To evaluate their potential use as vaccine candidates, we compared the immunological response of WRSs2E and WRSf2G12E to their parental strains in a mouse model. As mice do not experience diarrheal episodes from ingestion of *Shigella*, we evaluated vaccine efficacy through the generation of *Shigella*-specific immunological responses. Using three routes of vaccination (oral, intranasal, and intramuscular) and two different types of vaccines (live bacteria or purified LPS) (Fig. S8A), we determined that intranasal administration of live bacteria at Day 0, 14, and 28 (prime-boost-boost, respectively) generated the most reliable serum antibody response against serotype-specific LPS (Fig. S8B). Using this intranasal approach and the same vaccination scheme of prime-boost-boost at Day 0, 14, and 28, respectively, we showed that vaccination with WRSs2E or WRSf2G12E elicited strong serum IgG and IgA responses against serotype-specific LPS, that mimicked the response from their parental strains (Fig. 5A, B). Although statistically significant differences in antibody titers were observed between the parental and LpxE-modified strains at specific time points, these differences did not remain throughout the entire vaccine study. At Day 56, four weeks after the final vaccine dose was delivered, the skewing of IgG subclasses 2a and 1 was similar for WRSs2E and WRSf2G12E compared to their parental strains (Fig. 5C). The same
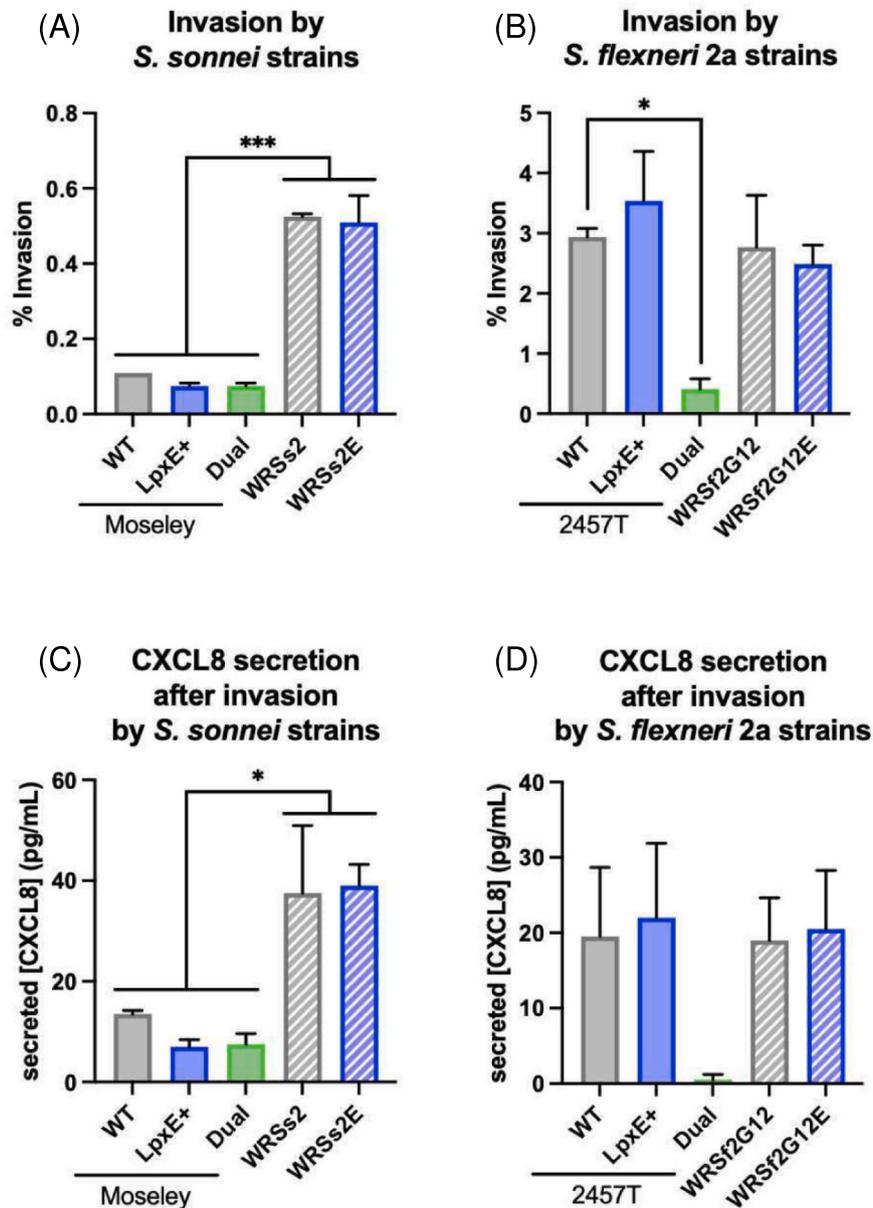
Fig. 3. Invasion of epithelial cells by *Shigella* and corresponding CXCL8 production. Invasion of HT29 cells after 4 h of infection (MOI of 10) with (A) *S. sonnei* and (B) *S. flexneri* 2a strains. CXCL8 production in the cell supernatant after the 4 h infection with (C) *S. sonnei* and (D) *S. flexneri* 2a strains. Statistical significance determined by ordinary one-way ANOVA. * and *** represent p-values of less than or equal to 0.05 and 0.001, respectively.

patterns were observed in a second independent vaccine study (Fig. S9). Ultimately, this data supports the notion that WRSs2E and WRSf2G12E promote a similar adaptive immune response as their parental strains.

3. Discussion

Despite significant advances in our understanding of *Shigella* pathogenesis and the development of many vaccine candidates [53], to date, there is no FDA-licensed vaccine available. This study utilized second-generation vaccine candidates WRSs2 and WRSf2G12, whose first-generation strains were generally well tolerated in clinical trials but deemed too reactogenic to be considered safe for general use [37,42]. These second-generation vaccine strains contain a suite of genetic manipulations that remove known enterotoxins and reduce the spread of the bacterium across gut epithelia [28,30,33]. In this study, we describe the engineering and characterization of an additional modification, specifically the dephosphorylation of their lipid A structure, to generate

WRSs2E and WRSf2G12E, which have reduced endotoxicity while retaining the same phenotypic traits as their isogenic parental strains.

The lipid A modifications engineered in this study utilized the BECC approach whereby prior identification of lipid A modifying enzymes from a variety of Gram-negative bacteria then enabled the expression of select enzymes within a bacterium of interest. Previously, the BECC system had been employed to generate custom-designed lipid A molecules in *Yersinia* [54–60]; however, this study extends its use to *Shigella* species, suggesting it is applicable to a variety of Gram-negative bacteria. More specifically, we showed that BECC enabled robust lipid A modification in both WT and vaccine strains of *Shigella*. Whereas multiple lipid A related spectral peaks were present upon plasmid-based expression of BECC constructs (Fig. S1), chromosomal expression generated a single spectral peak (Fig. 2) indicative of more complete lipid A modification on the outer membrane. This demonstrates a newfound approach for the expression of BECC enzymes since here we showed that chromosomally expressing strains are both stable and
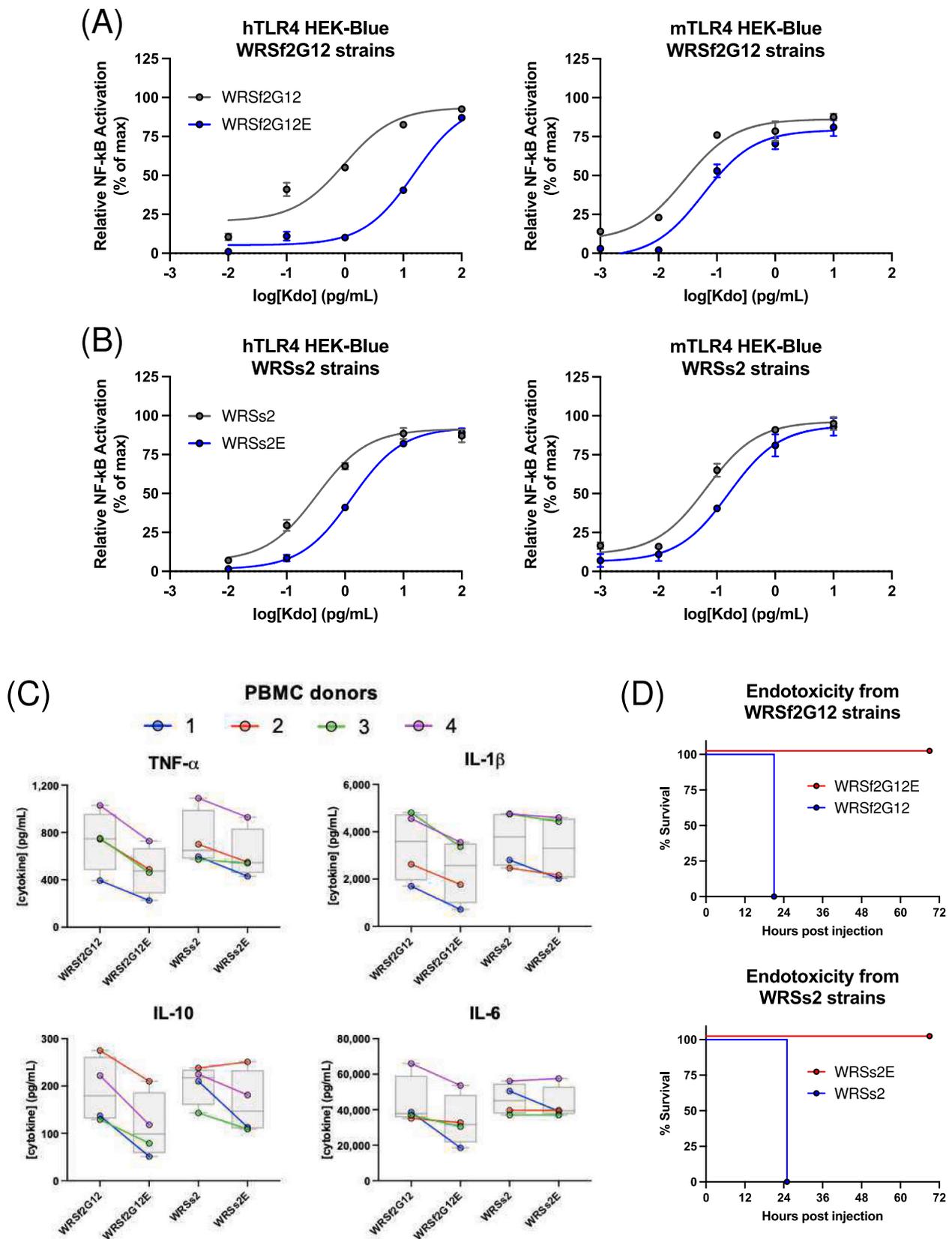
Fig. 4. Endotoxicity of BECC-modified LPS from WRSs2 and WRSf2G12 *in vitro* and *in vivo*. HEK 293 NF-kB reporter cells (HEK-Blue) overexpressing the human (hTLR4) or mouse (mTLR4) orthologs of TLR4/MD-2/CD-14 were stimulated across 10-fold dilutions, in duplicate, of Kdo standardized LPS from (A) WRSf2G12 and WRSf2G12E or (B) WRSs2 and WRSs2E for 18 h at 37 degrees celsius with 5% CO_2. (C) Human PBMCs from four independent donors, plotted as lines for each donor, were stimulated with 1 pg/mL of Kdo normalized LPS for 48 h at 37 degrees celsius with 5% CO_2 and cytokine levels in the supernatant quantified by multiplex analysis. The LPS used was purified from the indicated strains below the x-axis. (D) Survival curves for mice (n=5) receiving a Kdo normalized dose of LPS intraperitoneally, respresentative of 15 mg/kg, using purified LPS from the indicated strains.
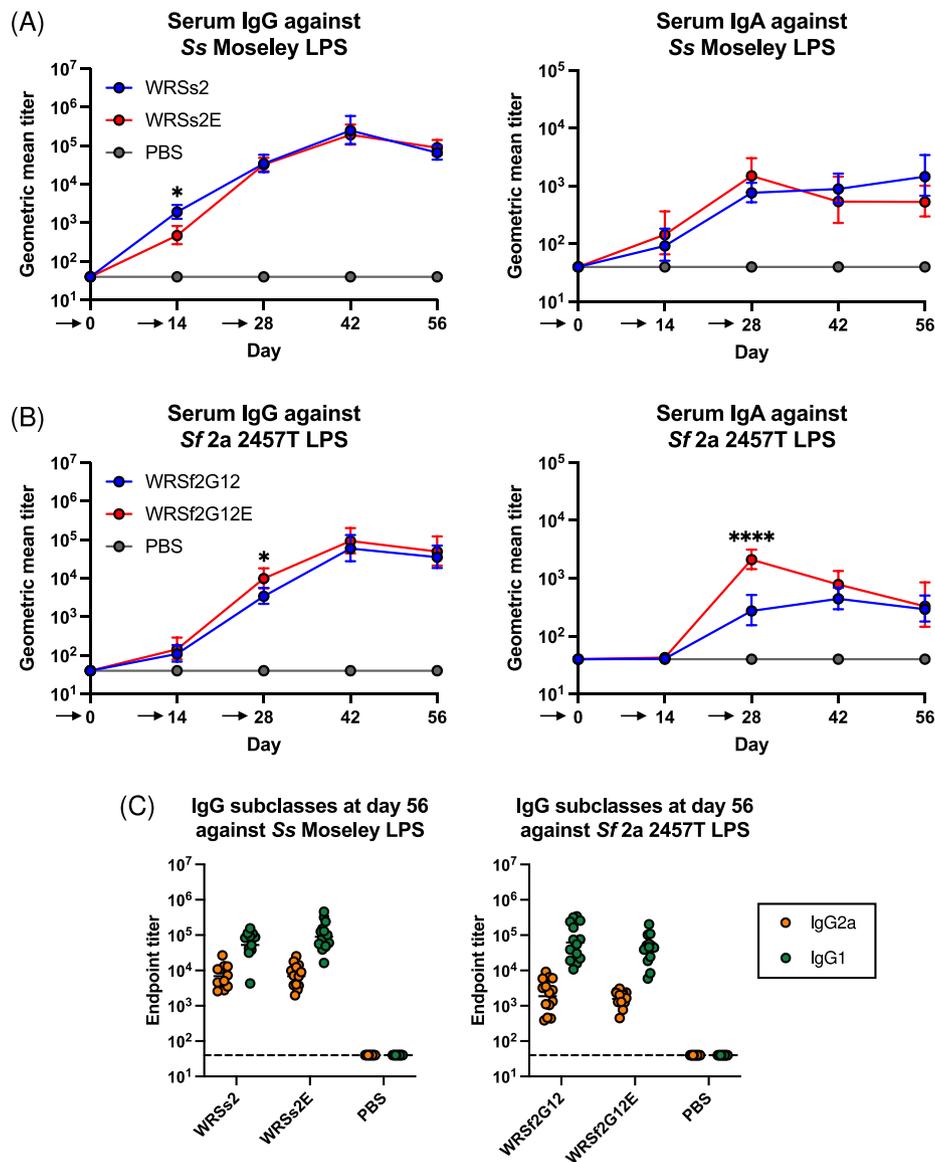
Fig. 5. Antibody titers from a *Shigella* murine vaccine study. Serum IgG and IgA geometric mean titers against (A) Moseley or (B) 2457T LPS for mice (n=15) vaccinated intranasally with 10^6 CFU at day 0, 14, and 28 as indicated by the arrows below the x-axis. (C) Serum IgG2a and IgG1 titers at day 56 against serotype-specific LPS. Statistical significance was determined by 2way ANOVA. * and **** represent p-values of less than or equal to 0.05 and 0.0001, respectively.

robustly modify their lipid A, all without the requirement for antibiotic selection.

Furthermore, to function as an effective oral vaccine, specific phenotypic requirements are required that may be altered upon engineering modified lipid A strains. We showed that dephosphorylation of lipid A had no impact on invasion or growth; however, Dual-modification (both dephosphorylation and deacylation) caused *S. flexneri* 2a 2457T to lose its invasion plasmid more frequently, likely a consequence of increased membrane stress. This is further supported by the inability to chromosomally integrate the Dual construct into WRSs2 or WRSf2G12, suggesting a limit to the degree to which lipid A can be modified in already genetically attenuated strains.

Additionally, we showed that dephosphorylation of lipid A at the 1-position *via* LpxE was sufficient to effectively blunt the LPS-induced pro-inflammatory response from both human and murine immune cells. This is analogous to other contexts, such as sepsis, where human alkaline phosphatase dephosphorylates LPS to reduce inflammatory signaling [61]. Traditionally, however, it is thought that deacylation of lipid A reduces LPS-induced TLR4/MD-2 signaling as tetra- and penta-acylated structures are generally less immunostimulatory than hexa-acylated

structures [46]. Here, we showed that PagL-mediated lipid A deacylation in *Shigella* at the 3-position did not greatly reduce LPS-mediated signaling (Fig. S2). Conversely, it has been shown that different penta-acylated *Shigella* lipid A structures, other than the one generated in this study, do in fact diminish LPS-induced signaling. Rossi et al., showed that an *htrB* mutant in *S. sonnei*, whose lipid A lacks the secondary acyl chain at the 2'-position, reduced TLR4 signaling in NF-κB reporter cells; however, the same mutation in *S. flexneri* 2a led to a compensatory C16:1 addition and no reduction in signaling compared to WT LPS [21]. This suggested that detoxification of *Shigella* lipid A *via* deacylation is site-specific. Furthermore, it emphasizes the complexity of achieving complete lipid A deacylation *via* genetic manipulation in *Shigella*. For instance, *Shigella* contains two *msbB* genes (both encoding MsbB/LpxM), one chromosomal and one on its invasion plasmid [62,63,74]. Additionally, *Shigella* can induce *lpxP* (encodes LpxP, C16:1 acylase) in the absence of *htrB* (encodes HtrB/LpxL) under stress-inducing conditions [49,64,65]. Altogether, this genetic redundancy of lipid A biosynthetic enzymes in *Shigella* highlights its drive to maintain hexa-acylated lipid A. Using BECC avoids this complication, as it introduces exogenous lipid A modifying enzymes and prevents induction

of compensatory mechanisms that revert its lipid A back to the hexa-acylated state. This is emphasized in the present study as primarily a single spectral peak was observed in the MALDI-TOF MS spectra upon expression of BECC constructs across the various *Shigella* backgrounds (Fig. 2), suggesting that the outer membrane contains predominantly the targeted lipid A structure without any compensatory lipid A modifications.

Despite remodeling of the lipid A region of LPS in the WRSs2E and WRSf2G12E, murine vaccination with these strains generated similar immune responses to their isogenic parental strains (Fig. 5 and S9). This suggested that serotype-specific immunity in response to vaccination with these strains was unaffected by BECC modification. Since *Shigella* does not cause diarrheal disease upon ingestion in rodents, only immunological responses were evaluated in this study; however, the first-generation variants of WRSs2 (WRSS1) and WRSf2G12 (SC602) have shown efficacy against shigellosis in humans [26,40]. Since LpxE-modification abrogates the toxic effects of LPS and does not appear to impact immunogenicity, this supports the notion that oral vaccination in humans with WRSs2E and WRSf2G12E would have reduced reactogenicity while maintaining robust immunogenicity and protection against shigellosis.

Overall, the need for a *Shigella* vaccine remains a priority. While it has been proposed that endemic *Shigella* can be controlled *via* public health efforts, the low infectious dose combined with its capacity to acquire extreme drug resistance has bolstered vaccination as a promising option to control the spread of this pathogen. To date, live-attenuated *Shigella* vaccines have shown immunological success in humans and, in some cases, protection against virulent challenges; this suggests that optimization of current live-attenuated vaccine candidates is a promising approach. A significant drawback with live-attenuated vaccine candidates, however, is the adverse effects from ingestion of high doses of bacteria containing the immunostimulatory hexa-acylated *Shigella* LPS. The BECC-modified vaccine strains of *Shigella* developed in this study, namely WRSs2E and WRSf2G12E, contain detoxified LPS and thus have promise to be better tolerated, safer, live-attenuated vaccine candidates.

4. Methods

4.1. Ethics statement

All animal procedures were approved by the University of Maryland, Baltimore Institutional Animal Care and Use Committee (IACUC #0222002). In all studies, female BALB/cJ mice (Jax Laboratories) were utilized. Mouse husbandry was conducted according to the procedures established at the University of Maryland, Baltimore.

4.2. Bacterial strains and growth conditions

Bacterial strains used in these studies are listed in Table S1. Bacteria were grown at 30°C or 37°C in Lysogenic Broth (Teknova) and Tryptic Soy broth (TSB) or on Tryptic Soy agar (TSA) (Becton Dickinson) supplemented with 50 µg/mL neomycin (Sigma) or 60 µg/mL carbenicillin (Sigma) as needed. All strains were supplemented with 1 mM MgCl$_2$ to repress the PhoPQ two-component regulatory system. Growth curves were performed in a flat-bottom 96-well uncoated sterile plate (Costar) and recorded using a Cerillo Stratus instrument (Cerillo). Each well was inoculated with 10^5 CFU in 200 µL TSB and incubated with shaking (180 RPM), at 37°C for 15 h. Absorbance readings at 600 nm were taken every 15 min.

4.3. Molecular genetic techniques

Standard DNA techniques, liquid media, and agar plates were used as described [66]. Restriction endonucleases and T4 DNA ligase were used as recommended by the manufacturer (New England Biolabs). DNA used for cloning purposes was PCR amplified using 10 mM dNTP mix (Thermo Scientific) and high-fidelity DNA polymerases Q5 (New England Biolabs) or Pfu ultra II fusion HS (Agilent) according to manufacturer's instructions. Go-Taq polymerase (Promega) was used for genetic screening. DNA oligonucleotides were obtained from Integrated DNA Technologies and are listed in Table S2. All plasmid constructs (Table S3) were confirmed by double-stranded sequencing (Azenta) and maintained in *E. coli* DH5α or *E. coli* TOP10 (ThermoFisher).

4.4. Generation of plasmid-based BECC-modified Shigella strains

LPS modifying enzymes LpxE, PagL, and LpxE-PagL in tandem (termed "Dual") were first cloned and expressed in pSEC10 [67] under the osmotically controlled *E. coli ompC* promoter (P$_{ompC}$). A codon-optimized form of *lpxE* from *Francisella novicida* was synthesized by GenScript and cloned into pUC57, yielding pUC57::*lpxE*. The 720 bp *lpxE* gene was amplified by PCR from pUC57::*lpxE* using Q5 polymerase (New England Biolabs) and primer set *lpxE*-F/*lpxE*-R, trimmed with restriction enzymes BamHI and NheI, and ligated into the BamHI/NheI site of pSEC10 resulting in the construct pSEC10::P$_{ompC}$-*lpxE*. The *pagL* gene was amplified by PCR from *Salmonella minnesota* (Genbank accession AE006468.2) using Q5 polymerase and primer set *pagL*-F/*pagL*-R. A 570 bp amplicon was trimmed with BamHI and NheI and ligated into the 6630 bp BamHI/NheI digested fragment of pSEC10 yielding pSEC10::P$_{ompC}$-*pagL*. Both *lpxE* and *pagL*, each preceded by a ribosomal binding site, were synthesized in tandem behind P$_{ompC}$ and cloned into vector pUC57K by GenScript yielding pUC57K::P$_{ompC}$-Dual. The initial subcloning of *pagL* into pSEC10 included six additional bps (GTGTAT) that encoded an alternative start codon present in the *S. minnesota* sequence; this 6 bp sequence was not included in the Dual construct. The P$_{ompC}$-Dual gene cassette was then cloned into a modified version of pSEC10 (pSEC10M). Briefly, primer set pSEC10M-F/pSEC10M-R was self-annealed, trimmed with EcoRI/NheI, and ligated into a 5775 bp gel purified EcoRI/NheI digested pSEC10 and transformed into *E. coli* TOP10. The resulting pSEC10M had a multiple cloning site [EcoRI-NotI-SwaI-NheI] in place of the *ompC* promoter and *clyA* gene. The 1.9 kb SwaI P$_{ompC}$-Dual gene cassette isolated from pUC57K::P$_{ompC}$-Dual was ligated into the SwaI digested site of pSEC10M and transformed into *E. coli* TOP10 yielding construct pSEC10M::P$_{ompC}$-Dual. Plasmids pSEC10::P$_{ompC}$-*lpxE*, pSEC10::P$_{ompC}$-*pagL*, and pSEC10M::P$_{ompC}$-Dual were electroporated into the wild-type strains of *S. sonnei* and *S. flexneri* 2a and selected on TSA with neomycin. Successful transformants were used to inoculate a 2 mL overnight culture in TSB with neomycin, which received a final concentration of 15% glycerol, followed by storage at −80°C.

4.5. Generation of attTn7 chromosomally integrated BECC-modified Shigella strains

We mobilized P$_{ompC}$-*lpx*E and P$_{ompC}$-Dual into the *Shigella* chromosome *attTn7* site using a site-specific insertion method utilizing the Tn7 recombination machinery on a temperature-sensitive plasmid pGRG36 [51]. A 1225 bp amplicon of the P$_{ompC}$-*lpxE* gene cassette was generated using template pSEC10::P$_{ompC}$-*lpxE*, Q5 polymerase (New England Biolabs) and primer set P$_{ompC}$-F/*lpxE*-R. This was then blunt-ligated into the SmaI digested site of pGRG36, yielding pGRG36::P$_{ompC}$-*lpxE*. A 1.9 kb P$_{ompC}$-Dual gene cassette flanked by SwaI restriction sites was isolated from pUC57K::P$_{ompC}$-Dual and ligated into the SwaI site of pGRG36 yielding pGRG36::P$_{ompC}$-Dual. The resulting pGRG36 constructs were transformed into *E. coli* S17–1 and introduced into wild-type and 2nd generation vaccine strains of *S. sonnei* and *S. flexneri* 2a by conjugal mating. Briefly, 2 mL cultures were grown overnight. *E. coli* S17–1 plasmid transformants were grown in the presence of carbenicillin at 30°C whereas *Shigella* cultures were grown without antibiotic at 37°C. Filter matings were performed by mixing 100 µL of *Shigella* with 50 µL of *E. coli* S17–1 plasmid transformants, concentrated by centrifugation (8k

x g for 1 min), resuspended in 200 μL TSB, spread onto a 0.45 μM nylon filter (MSI Magna nylon 66) placed on the center of a TSA plate, and incubated for 5 h at 30°C. Bacteria on the nylon filter were then resuspended in 1 mL TSB and plated onto TSA containing 0.01% Congo red dye (Sigma- Aldrich), carbenicillin, and 1 mM MgCl₂ and incubated overnight at 30°C. *Shigella* conjugants that grew at 30°C and were carbenicillin resistant were screened by PCR for the presence of *lpxE* and the *Shigella* invasion plasmid using GoTaq (Promega) using primer sets *lpxE*-F/*lpxE*-R and *ospD3*-F/*ospD3*-R or *lpxE*-F/*lpxE*-R and *ipaB*-F/*ipaB*-R for WT and vaccine strains, respectively. Bacteria were plated on TSA containing 0.1% arabinose and incubated at 42°C overnight to promote Tn7 recombination and simultaneous curing of pGRG36. Isolates that were carbenicillin sensitive and Congo Red positive, were assayed by PCR for the presence of *lpxE* using primer set *lpxE*-F/*lpxE*-R and for the *Shigella* invasion plasmid using ospD3 primer set *ospD3*-F/*ospD3*-R or *ipaB* primer set *ipaB*-F/*ipaB*-R for WT and vaccine strains, respectively. Confirmed integrants were stored in 15% glycerol at −80°C. Bacterial genomes were sequenced at the Microbial Genome Sequencing Center (SeqCenter) and analyzed using the RAST software [68] which confirmed the insertion of the gene cassettes into the *attTn7* site.

4.6. MALDI-TOF MS and MS/MS analysis of lipid A

Functional screening of *Shigella* strains to confirm lipid A modification was performed using the Fast Lipid Analysis Technique (FLAT) coupled to MALDI-TOF MS analysis [69]. Briefly, a single colony was spotted on a MALDI plate and overlaid with 1 μL of citrate buffer (200 mM citric acid, 100 mM trisodium citrate, pH 3.5). The plate was incubated in a humidified, closed, glass chamber for 30 min at 110°C, cooled, washed with endotoxin-free water, and 1 μL of 10 mg/mL norharmane matrix (Sigma-Aldrich) dissolved in chloroform: methanol (2:1 v/v) was spotted onto the samples on the MALDI plate. MALDI-TOF MS analysis was performed using a Bruker Microflex LRF equipped with a 337 nm nitrogen laser. Spectra were acquired in the negative ion and reflectron mode. Analyses were conducted at <60% global intensity with 300 laser shots for each spectrum acquisition. Spectra were recorded in triplicate. Agilent ESI tune mix (Agilent) was used for mass calibration. FlexAnalysis software version 3.4 (Bruker) was used to process the mass spectra with smoothed and baseline corrections. Further structural lipid A characterization was conducted by tandem mass spectrometry (MS/MS) analysis using the FLAT^n procedure [52]. The FLAT process above was repeated, except the colony spotted onto an indium tin oxide (ITO) slide instead of a MALDI plate. MS/MS analysis was performed using a Bruker MALDI trapped ion mobility spectrometry Time-of-Flight (timsTOF) mass spectrometer equipped with a dual ESI/MALDI source with a SmartBeam 3D 10 KHz frequency tripled 355 nm Nd:YAG laser. The system was operated in "qTOF" mode (tims deactivated). Ion transfer tuning used the following parameters: Funnel 1 RF: 440.0 Vpp, Funnel 2 RF: 490.0 Vpp, Multipole RF 490.0 Vpp, is CID Energy: 0.0 eV, and Deflection Delta: −60.0 V. The quadrupole used the following values for MS mode: Ion Energy: 4.0 eV and Low Mass 700.00 *m/z*. Collision cell activation of ions used the following values for MS mode: Collision Energy: 9.0 eV and Collision RF: 3900.0 Vpp. The precursor ion was chosen by inputting targeted *m/z* values including two digits beyond the decimal point. Typical isolation width and collision energy were set to 4–6 *m/z* and 100–110 eV, respectively. Focus Pre-TOF used the following values: Transfer time 110.0 μs and Pre pulse storage 9.0 μs. Agilent ESI Tune Mix (Agilent) was used to perform calibration. MALDI parameters in qTOF mode were optimized to maximize intensity by tuning ion optics, laser intensity, and laser focus. All spectra were collected at a laser diameter of 104 μm with beam scan on using 800 laser shots per spot using either 70% or 80% laser power. MS/MS data were collected in negative ion mode. In all cases, a matrix of 10 mg/mL norharmane dissolved in chloroform: methanol (2:1 v/v) was used. mMass software version 5.5.0 [70] was used to process the mass spectra with smoothed and baseline corrections. Identification of all fragment ions were determined based on ChemDraw Ultra version 10.0.

4.7. SDS-PAGE and Pro-Q Emerald 300 staining

LPS was isolated from small-scale (2 mL) cultures *via* hot aqueous-phenol extraction according to [71] and separated by SDS-PAGE on NuPAGE 4–12% Bis-Tris precast gels (Invitrogen) at 150 V for 35 min. The gel was fixed and stained according to the Pro-Q™ Emerald 300 Lipopolysaccharide Gel Stain Kit manufacturers protocol (Invitrogen) and exposed for 0.5 s using the Pro-Q Emerald 300 filter on a standard ChemiDoc imaging system (Bio-Rad).

4.8. LPS extraction and purification

LPS was isolated using the double hot phenol method. Briefly, two liters of bacterial culture were harvested by centrifugation and resuspended in 90% phenol: endotoxin-free water (1:1 v/v) and incubated at 65°C for 1 h. After centrifugation, the aqueous phase was isolated from the two-phase solution (repeated three times total and pooled) and dialyzed for 36 h against deionized water using pre-treated 1 kD MWCO RC tubing (Spectrumlabs.com), followed by flash freezing and lyophilization. The lyophilized product was resuspended in 20 mM Tris-HCl pH 8.4 supplemented with 2 mM MgCl₂ and digested using 500 units of Benzonase and 100 μg/mL Dnase I for 2 h at 37°C. The pH was subsequently adjusted to 7.4 using 1 N HCl and the solution further digested with 100 μg/mL Proteinase K for 2 h at 37°C. Water-saturated phenol was added, vortexed, and centrifuged (8,000 x*g*), and the upper aqueous phase was collected, dialyzed, and lyophilized. Further isolation of LPS was performed by serial washes in chloroform: methanol (2:1 v/v) as described [72]. The LPS was separated from contaminating lipoproteins as described [73] by resuspension in 0.2% TEA (triethylamine) and 0.5% DOC (deoxycholate), followed by the addition of 37°C water-saturated phenol and the upper aqueous phase collected. Finally, the LPS product was precipitated by the addition of cold 100% ethanol and 30 mM sodium acetate followed by incubation for 18 h at −20°C. The LPS precipitate was harvested by centrifugation (5,000 x*g*, 20 min), washed in cold 100% ethanol, resuspended in endotoxin-free water (Quality Biological), and lyophilized.

4.9. Kdo assay for LPS quantification

2-keto-3-deoxyoctonate (Kdo) standards ranging from 12 to 48 μg/mL in endotoxin-free water and 1 mg/mL LPS solution solutions were hydrolyzed in 0.018 N sulfuric acid (H₂SO₄) at 100°C for 20 min, followed by the addition of 25 μL of 9.1 mg/mL periodic acid (H₅IO₆) in 0.125 N H₂SO₄ and incubation in the dark for 20 min. Samples then received 50 μL of 2.6% sodium arsenite (NaAsO2) in 0.5 N HCl followed by the addition of 250 μL of 0.3% thiobarbituric acid (TBA). Samples were heated at 100°C for 10 min, quickly followed by the addition of 125 μL of dimethyl sulfoxide (DMSO), and the measurement of absorbance at 550 nm. The absolute quantification is based on the interpolation of the standard curve provided by the Kdo₂ quantity. Half of the Kdo₂ quantity, representing Kdo₁ (referred to as simply "Kdo" in this study), was utilized for normalization.

4.10. Murine acute endotoxemia

LPS solutions of 45 μg/mL Kdo₂ (representative of 15 mg/kg if using dry weight instead) were prepared in sterile, endotoxin-free PBS (Quality Biology). LPS solutions were transferred to arbitrarily labeled tubes by a third-party observer to ensure blinding to group identifications and avoid bias in clinical score designations. Each mice received 100 μL of LPS solution using a slip tip 1 mL syringe attached to a 27-gauge ½ inch needle (Becton Dickinson) *via* the intraperitoneal route. Mice were monitored for 72 h post-injection, receiving a clinical score/mouse based on appearance and mobility as described in Table S4. A

clinical score of 5 required euthanization as a consequence of no movement, noticeable stress, and an inability to return upright if placed on their side.

4.11. Cell culture media and conditions

RPMI-1640 (Gibco) complemented with 25 mM HEPES, 2 mM glutamine, 10% FBS, and 1% penicillin-streptomycin, referred to as cRPMI, was filter sterilized through a 0.22 μM filter flask and used for the THP-1 NF-κB-SEAP reporter cell line (THP-1 Dual, Invitrogen). DMEM (Corning) complemented with 3.7 g/L sodium bicarbonate, 2 mM glutamine, 10% FBS, and 1% penicillin-streptomycin, referred to as cDMEM, was filter sterilized through a 0.22 μM filter flask and used for the HT29 cells (courtesy of Dr. Eileen Barry, UMB), mTLR4/hTLR4 HEK-Blue cells (Invitrogen), and RAW-Blue cells (Invitrogen). All cells were maintained at 37°C with 5% CO_2.

4.12. NF-κB reporter cell line stimulations

Sterile, cell culture-treated, 96-well flat bottom plates (Costar) were seeded with HEK-Blue, RAW-Blue, or THP-1 Dual reporter cells at 6×10^4 cells/well. THP-1 cells received 100 ng/mL of vitamin D_3 (Sigma) prior to seeding in wells to enable cell differentiation. Cells were incubated for 18 h at 37°C with 5% CO_2, except the THP-1 cells, which were incubated for 72 h to enable differentiation into monocyte-derived macrophages. Five 10-fold dilutions of Kdo standardized LPS ranging from 10^2 pg/mL to 10^{-2} pg/mL was used to stimulate NF-κB production in cells. Cells were incubated at 37°C with 5% CO_2 for 18 h. Detection of NF-κB was quantified using the Quanti-Blue (QB) reagent prepared according to the manufacturer's protocols (Invitrogen). The percent of relative NF-κB activation was normalized to the maximum OD 630 nm measured. Points were plotted as the mean ± standard deviation of the relative NF-κB activation at each concentration using GraphPad Prism version 9 and fitted using a nonlinear regression of the log(agonist) *versus* response (three parameters).

4.13. Stimulation of primary peripheral blood monocytes

Human peripheral blood was collected from healthy adult study participants 18–40 years of age per a Boston Children's IRB-approved protocol (protocol number X07-05-0223). All participants signed an informed consent form prior to enrollment. Heparinized whole blood was centrifuged (500 x*g*, 10 min) prior to removal of the upper layer of platelet-rich plasma. The plasma was centrifuged (3,000 x*g*, 10 min) and platelet-poor plasma (PPP) was collected and stored on ice. The remaining blood was reconstituted to its original volume with heparinized Dulbecco's PBS and layered on Ficoll-Paque gradients (Cytiva) in Accuspin tubes (Sigma-Aldrich). PBMCs were collected after centrifugation, washed twice with PBS, and seeded at 2×10^5 cells/well in 96-well U-bottom plates (Corning) in RPMI-1640 media (Gibco) supplemented with 10% autologous PPP, 100 IU/ mL penicillin, 100 μg/mL streptomycin, and 2 mM L-glutamine. PBMCs were incubated with 1 pg/ mL Kdo standardized LPS for 24 h at 37 °C with 5% CO2. The supernatants were recovered after centrifugation (500 x*g*, 5 min) and analyzed for TNF-α quantification.

For multiplex analysis, frozen PBMCs from 4 independent human donors were instead obtained from AllCells, snap-thawed, washed twice with warm cRPMI, and seeded at 5×10^5 cells/well in 96-well, sterile, uncoated U-bottom plates (Costar). PBMCs were incubated with 1 pg/ mL Kdo standardized LPS for 48 h at 37 °C with 5% CO2. The supernatants were recovered after centrifugation (400 x*g*, 5 min) and stored at −20°C until analyzed by MSD multiplex.

4.14. Invasion assays

HT29 cells were seeded at a density of 5×10^5 cells/well in 24-well flat bottom sterile plates (Corning) and incubated at 37°C for 18 h with 5% CO_2. *Shigella* cultures from overnight growth on TSA containing 0.01% Congo Red were used to generate a resuspension in sterile PBS pH 7.4. Inoculums of 5×10^6 CFU in serum free media were used to infect, giving an MOI of 10. Enumeration of the inoculation was confirmed in duplicate by plate counts on TSA. Bacterial inoculums were added to PBS-washed cell monolayers and the plates were centrifuged (3,000 x*g*, 5 min) to start the infection. After incubation for 90 min at 37°C with 5% CO_2, cell monolayers were twice washed with sterile PBS, followed by the addition of cDMEM containing 50 μg/mL gentamycin (Sigma-Aldrich) and incubation for 2.5 h. Supernatants were isolated and processed for human CXCL8 secretion by cytokine ELISA. The cell monolayer was twice washed with sterile PBS and lysed with 1% Triton X-100 (Sigma-Aldrich) in sterile PBS for 10 min at room temperature. Serial dilutions were plated in duplicate on TSA and incubated overnight at 37°C. The percentage of invasion was determined as the CFU/mL recovered normalized to the CFU/mL inoculated.

4.15. Cytokine ELISA

Cytokine analysis of host cell culture supernatants was performed using DuoSet ELISA kits (R&D Systems) according to the manufacturer's protocol. Briefly, plates were coated overnight at 4°C by adding 100 μL/ well of 2 μg/mL capture antibody in ELISA coating buffer, washed three times PBS + 0.02% Tween-20 (PBST) and blocked with 300 μL/well 1% BSA in PBS for 1 h at room temperature followed by three washes with PBST. Cell culture supernatants were diluted to reach a signal within the dynamic range. Bound cytokines were labeled by adding biotin-conjugated antibodies in block buffer (100 μL/well of 2 pg/mL) and incubated at room temperature for 2 h. Plates were washed with PBST and incubated for 20 min with secondary antibody streptavidin-HRP, followed by the addition of a color substrate. The plates were read at both 450 nm and 562 nm and the difference taken as the final reading. The amount of cytokine is reported as picograms per mL of cell culture supernatant.

4.16. Murine vaccination with live-attenuated Shigella

Shigella vaccine strains were grown at 37°C overnight on TSA containing 0.01% Congo Red. For intranasal vaccination, inoculums of 3.33 $\times 10^8$ CFU/mL and 3.33 $\times 10^7$ CFU/mL of *Shigella* were prepared in sterile PBS and kept at room temperature. Mice were anesthetized using a Matrx VIP 3000 vaporizer (Midmark Animal Health) with isoflurane (Fluriso, VetOne): oxygen (Airgas, OX USPEAWBDS) mixture (1:1 mixing) for 1–2 min and 15 μL of the vaccine inoculum was delivered to each nare (30 μL in total) using a pipette. For oral gastric vaccination, inoculums of 1×10^8 CFU/mL and 1×10^7 CFU/mL of *Shigella* were prepared in sterile PBS and kept at room temperature. Inoculums of 100 μL were delivered by intra-gastric gavage using a 2-in.-long plastic feeding needle (VWR) connected to a 1 mL syringe (Becton Dickinson). For both vaccination methods, mice were monitored for adverse reactions post-immunization. Enumeration of the vaccine inoculums was determined by plate counts on TSA.

4.17. Murine vaccination with purified LPS

Purified LPS from wild-type *S. sonnei* Moseley was obtained as described above (see LPS extraction and purification). For internasal vaccination, solutions containing purified LPS at 1 mg/mL and 0.66 mg/ mL, dissolved in sterile PBS, were delivered intranasally as described above. For intramuscular vaccination, solutions containing purified LPS at 0.6 mg/mL and 0.4 mg/mL, dissolved in sterile PBS, were prepared and stored at room temperature. Mice were immobilized using a restrainer, and 50 μL of the solution was injected using a 1 mL syringe (Becton Dickinson) into the caudal muscle after disinfecting the area with 70% ethanol. For both vaccination methods, mice were monitored

for adverse reactions post-immunization.

4.18. Sera collection

Mice were bled *via* the lateral saphenous vein using petroleum jelly and 27-gauge needles. Blood was collected in a microvette 200 *Z*-gel tubes (Sarstedt), and the sera were isolated by centrifugation (10,000 x*g*, 3 min) and stored in sealed uncoated 96-well flat bottom plates (Thermo Fischer) at −20°C.

4.19. LPS ELISA

Coating antigens used in ELISAs included purified LPS from wild-type *S. sonnei* Moseley or *S. flexneri* 2a 2457T. Nunc MaxiSorp plates (ThermoFischer) were coated with 5 μg/mL serotype-specific LPS in 100 mM carbonate coating buffer pH 9.6 (sodium bicarbonate/carbonate) and incubated for 3 h at 37°C. Plates were washed with PBS containing 0.05% Tween-20 (Sigma) (PBST) and blocked with 10% non-fat dry milk powder (Quality Biological) in PBST overnight at 4°C. Sera was diluted in 5-fold increments starting with a 1:50 dilution in PBST, added to the LPS-coated plates, and incubated at 37°C for 2 h. Plates were washed with PBST. Incubation for 1 h with secondary HRP-conjugated antibodies, goat anti-mouse IgG, IgG1, IgG2a (Southern Biotech) or goat anti-mouse IgA (Invitrogen) was followed by a 15 min room temperature incubation with 3,3′,5,5′-tetramethylbenzidine (TMB) substrate (BD biosciences) prepared according to manufacturer's protocol. KPL TMB stop solution (Sera Care) containing 1% HCl was added to each well, and the absorbance read at 450 nm. The endpoint titer was determined as the absorbance reading that was equal to the reciprocal dilution required for the signal to match the average blank (PBST alone, no sera). Samples were run in duplicate. Sera from days 28, 42, and 56 of the vaccine study required dilutions of 1:1250 for IgG and IgG1 titers and 1:250 for IgG2a to reach specific endpoints.

4.20. Multiplex cytokine analysis

MSD (Meso Scale Development) V-PLEX human proinflammatory panel 1 (10-plex) was used for the analysis of the human orthologs of IFNγ, IL-1β, IL-2, IL-4, IL-6, CXCL8, IL-10, IL-12p70, IL-13 and TNF-α from 25 μL of 6-fold dilutions of the supernatant from the stimulation of human PBMCs; however only data from IL-1β, IL-6, IL-10, and TNF-α were used for this study. Samples and calibrators were incubated at room temperature, shaking (500 RPM), for 2 h. Plates were washed with PBST and MSD detection antibody solution, prepared according to the manufacturer's protocol, added and incubated shaking (500 RPM) at room temperature for 2 h. Plates were washed with 150 μL/well PBST followed by the addition of 150 μL/well of read buffer T. Plates were immediately read on an MSD SQ 120/120MM instrument. Cytokine concentration was determined by interpolation from a standard curve generated using the provided calibrators.

CRediT authorship contribution statement

Matthew E. Sherman: Writing – review & editing, Writing – original draft, Visualization, Project administration, Methodology, Investigation, Formal analysis, Data curation. **Jane Michalski:** Writing – review & editing, Resources, Project administration, Methodology, Investigation, Funding acquisition, Formal analysis, Data curation. **Sayan Das:** Writing – review & editing, Methodology, Investigation. **Hyojik Yang:** Writing – review & editing, Methodology, Investigation. **Lakshmi Chandrasekaran:** Writing – review & editing, Resources, Project administration, Methodology, Investigation, Formal analysis, Data curation. **Timothy R. O'Meara:** Writing – review & editing, Validation, Investigation. **David J. Dowling:** Writing – review & editing, Supervision. **Ofer Levy:** Writing – review & editing, Supervision. **Shoshana Barnoy:** Writing – review & editing, Resources, Project administration, Methodology, Investigation, Funding acquisition. **Malabi Venkatesan:** Writing – review & editing, Supervision, Resources, Project administration, Methodology, Investigation, Funding acquisition, Conceptualization. **Robert K. Ernst:** Writing – Review & editing, Supervision, Resources, Porject administration, Methodology, Investigation, Funding aquisition, Conceptualization.

Declaration of competing interest

Appendix A. Supplementary data

Supplementary data to this article can be found online at https://doi.org/10.1016/j.vaccine.2025.126779.

Data availability

The datasets generated and analyzed during the current study are available from the corresponding author on reasonable request.

References

[1] Vos T, et al. Global, regional, and national incidence, prevalence, and years lived with disability for 310 diseases and injuries, 1990–2015: a systematic analysis for the global burden of disease study 2015. Lancet 2016;388(10053):1545–602.

[2] Wang H, et al. Global, regional, and national life expectancy, all-cause mortality, and cause-specific mortality for 249 causes of death, 1980–2015: a systematic analysis for the global burden of disease study 2015. Lancet 2016;388(10053):1459–544.

[3] Troeger C, et al. Estimates of the global, regional, and national morbidity, mortality, and aetiologies of diarrhoea in 195 countries: a systematic analysis for the global burden of disease study 2016. Lancet Infect Dis 2018;18(11):1211–28.

[4] Walker R, et al. Vaccines for protecting infants from bacterial causes of diarrheal disease. Microorganisms 2021;9(7):1382.

[5] Pasetti MF, Venkatesan MM, Barry EM. Oral Shigella Vaccines. In: Mucosal vaccines; 2020. p. 515–36.

[6] Liu J, et al. Use of quantitative molecular diagnostic methods to identify causes of diarrhoea in children: a reanalysis of the GEMS case-control study. Lancet 2016;388(10051):1291–301.

[7] Khalil IA, et al. Morbidity and mortality due to shigella and enterotoxigenic *Escherichia coli* diarrhoea: the global burden of disease study 1990–2016. Lancet Infect Dis 2018;18(11):1229–40.

[8] Williams PCM, Berkley JA. Guidelines for the treatment of dysentery (shigellosis): a systematic review of the evidence. Paediatrics Int Child Health 2018;38(sup1):S50–65.

[9] Anderson JD, et al. Burden of enterotoxigenic *Escherichia coli* and shigella non-fatal diarrhoeal infections in 79 low-income and lower middle-income countries: a modelling analysis. Lancet Glob Health 2019;7(3):e321–30.

[10] Schroeder GN, Hilbi H. Molecular pathogenesis of Shigella spp.: controlling host cell signaling, invasion, and death by type III secretion. Clin Microbiol Rev 2008;21(1):134–56.

[11] Kotloff KL, et al. Shigellosis. Lancet 2018;391(10122):801–12.

[12] Shad AA, Shad WA. Shigella sonnei: virulence and antibiotic resistance. Arch Microbiol 2021;203(1):45–58.

[13] Network, C.H.A. Increase in extensively drug-resistant shigellosis in the United States. 2023 February. 24, 2023; Available from: https://emergency.cdc.gov/han/2023/han00486.asp.

[14] Barry EM, et al. Progress and pitfalls in Shigella vaccine research. Nat Rev Gastroenterol Hepatol 2013;10(4):245–55.

[15] Levine MM, et al. Clinical trials of Shigella vaccines: two steps forward and one step back on a long, hard road. Nat Rev Microbiol 2007;5(7):540–53.

[16] Kaminski RW, Oaks EV. Inactivated and subunit vaccines to prevent shigellosis. Expert Rev Vaccines 2009;8(12):1693–704.

[17] Turbyfill KR, et al. Assembly, biochemical characterization, immunogenicity, Adjuvanticity, and efficacy of Shigella artificial Invaplex. mSphere 2018;3(2).

[18] Duplessis C, et al. GMP manufacture of *Shigella flexneri* 2a artificial Invaplex (Invaplex(AR)) and evaluation in a phase 1 open-label, dose escalating study administered intranasally to healthy, adult volunteers. Vaccine 2023;41(42):6261–71.

[19] Turbyfill KR, et al. Development of the Shigella flexneri 2a, 3a, 6, and S. sonnei artificial Invaplex (Invaplex(AR)) vaccines. mSphere 2023;8(4):e0007323.

[20] Berlanda Scorza F, et al. High yield production process for Shigella outer membrane particles. PLoS One 2012;7(6):e35616.

[21] Rossi O, et al. Modulation of Endotoxicity of Shigella generalized modules for membrane antigens (GMMA) by genetic lipid a modifications. J Biol Chem 2014;289(36):24922–35.

[22] Gerke C, et al. Production of a *Shigella sonnei* vaccine based on generalized modules for membrane antigens (GMMA), 1790GAHB. PLoS One 2015;10(8):e0134478.

[23] Conti V, et al. Putative correlates of protection against shigellosis assessing immunomarkers across responses to *S. sonnei* investigational vaccine. NPJ Vaccines 2024;9(1):56.

[24] Venkatesan MM, Ranallo RT. Live-attenuated Shigella vaccines. Expert Rev Vaccines 2006;5(5):669–86.

[25] Livio S, et al. Shigella isolates from the global enteric multicenter study inform vaccine development. Clin Infect Dis 2014;59(7):933–41.

[26] Coster TS, et al. Vaccination against shigellosis with attenuated *Shigella flexneri* 2a strain SC602. Infect Immun 1999;67(7):3437–43.

[27] Barzu S, et al. Induction of a local anti-IpaC antibody response in mice by use of a *Shigella flexneri* 2a vaccine candidate: implications for use of IpaC as a protein carrier. Infect Immun 1996;64(4):1190–6.

[28] Hartman AB, Venkatesan MM. Construction of a stable attenuated *Shigella sonnei* DeltavirG vaccine strain, WRSS1, and protective efficacy and immunogenicity in the guinea pig keratoconjunctivitis model. Infect Immun 1998;66(9):4572–6.

[29] Collins TA, et al. Safety and colonization of two novel VirG(IcsA)-based live *Shigella sonnei* vaccine strains in rhesus macaques (*Macaca mulatta*). Comp Med 2008;58(1):88–94.

[30] Barnoy S, et al. Characterization of WRSs2 and WRSs3, new second-generation virG(icsA)-based *Shigella sonnei* vaccine candidates with the potential for reduced reactogenicity. Vaccine 2010;28(6):1642–54.

[31] Barnoy S, et al. *Shigella sonnei* vaccine candidates WRSs2 and WRSs3 are as immunogenic as WRSS1, a clinically tested vaccine candidate, in a primate model of infection. Vaccine 2011;29(37):6371–8.

[32] Bedford L, et al. Further characterization of *Shigella sonnei* live vaccine candidates WRSs2 and WRSs3-plasmid composition, invasion assays and Sereny reactions. Gut Microbes 2011;2(4):244–51.

[33] Ranallo RT, et al. Two live attenuated *Shigella flexneri* 2a strains WRSf2G12 and WRSf2G15: a new combination of gene deletions for 2nd generation live attenuated vaccine candidates. Vaccine 2012;30(34):5159–71.

[34] Jeong K-I, et al. Evaluation of virulent and live *Shigella sonnei* vaccine candidates in a gnotobiotic piglet model. Vaccine 2013;31(37):4039–46.

[35] Ranallo RT, et al. Oral administration of live Shigella vaccine candidates in rhesus monkeys show no evidence of competition for colonization and immunogenicity between different serotypes. Vaccine 2014;32(15):1754–60.

[36] Kotloff KL, et al. Phase I evaluation of delta virG *Shigella sonnei* live, attenuated, oral vaccine strain WRSS1 in healthy adults. Infect Immun 2002;70(4):2016–21.

[37] Katz DE, et al. Two studies evaluating the safety and immunogenicity of a live, attenuated Shigella flexneri 2a vaccine (SC602) and excretion of vaccine organisms in north American volunteers. Infect Immun 2004;72(2):923–30.

[38] Orr N, et al. Community-based safety, immunogenicity, and transmissibility study of the *Shigella sonnei* WRSS1 vaccine in Israeli volunteers. Infect Immun 2005;73(12):8027–32.

[39] Rahman KM, et al. Safety, dose, immunogenicity, and transmissibility of an oral live attenuated Shigella flexneri 2a vaccine candidate (SC602) among healthy adults and school children in Matlab, *Bangladesh*. Vaccine 2011;29(6):1347–54.

[40] Pitisuttithum P, et al. Clinical trial of an Oral live *Shigella* vaccine candidate, WRSS1, in thai adults clinical and vaccine. Immunology 2016;23(7):564–75.

[41] Raqib R, et al. A phase I trial of WRSS1, a *Shigella sonnei* live oral vaccine in Bangladeshi adults and children. Hum Vaccin Immunother 2019;15(6):1326–37.

[42] Frenck RW, et al. A phase I trial to evaluate the safety and immunogenicity of WRSs2 and WRSs3; two live oral candidate vaccines against *Shigella sonnei*. Vaccine 2018;36(32):4880–9.

[43] Miller SI, Ernst RK, Bader MW. LPS, TLR4 and infectious disease diversity. Nat Rev Microbiol 2005;3(1):36–46.

[44] Chandler CE, Ernst RK. Bacterial lipids: powerful modifiers of the innate immune response. F1000Research 2017;6:1334.

[45] Zamyatina A, Heine H. Lipopolysaccharide recognition in the crossroads of TLR4 and Caspase-4/11 mediated inflammatory pathways. Front Immunol 2020;11:585146.

[46] Scott AJ, et al. Lipid a structural modifications in extreme conditions and identification of unique modifying enzymes to define the toll-like receptor 4 structure-activity relationship. Biochimica et Biophysica Acta (BBA) - molecular and cell biology of Lipids 2017;1862(11):1439–50.

[47] Park BS, et al. The structural basis of lipopolysaccharide recognition by the TLR4–MD-2 complex. Nature 2009;458(7242):1191–5.

[48] Raetz CRH, et al. Lipid a modification Systems in Gram-Negative Bacteria. Annu Rev Biochem 2007;76(1):295–329.

[49] Simpson BW, Trent MS. Pushing the envelope: LPS modifications and their consequences. Nat Rev Microbiol 2019;17(7):403–16.

[50] Ernst RK, Pelletier M, Hajjar A. Immunotherapeutic Potential of Modified Lipooligosaccharides/Lipid A. US Patent 2019;10:358,667.

[51] McKenzie GJ, Craig NL. Fast, easy and efficient: site-specific insertion of transgenes into Enterobacterial chromosomes using Tn7 without need for selection of the insertion event. BMC Microbiol 2006;6(1):39.

[52] Yang H, et al. Lipid a structural determination from a single Colony. Anal Chem 2022;94(21):7460–5.

[53] MacLennan CA, et al. The Shigella Vaccines Pipeline Vaccines (Basel)10; 2022. p. 9.

[54] Gregg KA, et al. Rationally designed TLR4 ligands for vaccine adjuvant discovery. mBio 2017;8(3):e00417–92.

[55] Gregg KA, et al. A lipid A-based TLR4 mimetic effectively adjuvants a *Yersinia pestis* rF-V1 subunit vaccine in a murine challenge model. Vaccine 2018;36(28):4023–31.

[56] Haupt RE, et al. Novel TLR4 adjuvant elicits protection against homologous and heterologous influenza a infection. Vaccine 2021;39(36):5205–13.

[57] Zacharia A, et al. Optimization of RG1-VLP vaccine performance in mice with novel TLR4 agonists. Vaccine 2021;39(2):292–302.

[58] Alexander-Floyd J, et al. Position-specific secondary acylation determines detection of lipid a by murine TLR4 and Caspase-11. Infect Immun 2022;90(8): e0020122.

[59] Harberts EM, et al. Lipid a variants activate human TLR4 and the noncanonical Inflammasome differently and require the Core oligosaccharide for Inflammasome activation. Infect Immun 2022;90(8):e0020822.

[60] Haupt R, et al. Enhancing the protection of influenza virus vaccines with BECC TLR4 adjuvant in aged mice. Sci Rep 2023;13(1):715.

[61] Pettengill M, et al. Human alkaline phosphatase dephosphorylates microbial products and is elevated in preterm neonates with a history of late-onset sepsis. PLoS One 2017;12(4):e0175936.

[62] D'Hauteville HLN, et al. Two msbB genes encoding maximal acylation of lipid a are required for invasive *Shigella flexneri* to mediate inflammatory rupture and destruction of the intestinal epithelium. J Immunol 2002;168(10):5240–51.

[63] Ranallo RT, et al. Virulence, inflammatory potential, and adaptive immunity induced by *Shigella flexneri* msbB mutants. Infect Immun 2010;78(1):400–12.

[64] Carty SM, Sreekumar KR, Raetz CR. Effect of cold shock on lipid a biosynthesis in *Escherichia coli*. Induction at 12 degrees C of an acyltransferase specific for palmitoleoyl-acyl carrier protein. J Biol Chem 1999;274(14):9677–85.

[65] Needham BD, Trent MS. Fortifying the barrier: the impact of lipid a remodelling on bacterial pathogenesis. Nat Rev Microbiol 2013;11(7):467–81.

[66] Sambrook J, Green MR, Molecular cloning : a laboratory manual. Cold Spring Harbor. N.Y: Cold Spring Harbor Laboratory Press; 2001.

[67] Stokes MG, et al. Oral administration of a *Salmonella enterica*-based vaccine expressing *Bacillus anthracis* protective antigen confers protection against aerosolized *B. anthracis*. Infect Immun 2007;75(4):1827–34.

[68] Aziz RK, et al. The RAST server: rapid annotations using subsystems technology. BMC Genomics 2008;9:75.

[69] Sorensen M, et al. Rapid microbial identification and colistin resistance detection via MALDI-TOF MS using a novel on-target extraction of membrane lipids. Sci Rep 2020;10(1).

[70] Niedermeyer THJ, Strohalm M. mMass as a software tool for the annotation of cyclic peptide tandem mass spectra. PLoS One 2012;7(9):e44913.

[71] Davis Jr MR, Goldberg JB. Purification and visualization of lipopolysaccharide from gram-negative bacteria by hot aqueous-phenol extraction. J Vis Exp 2012;63.

[72] Folch J, Lees M, Sloane Stanley GH. A simple method for the isolation and purification of total lipides from animal tissues. J Biol Chem 1957;226(1):497–509.

[73] Hirschfeld M, et al. Cutting edge: Repurification of lipopolysaccharide eliminates signaling through both human and murine toll-like receptor 2. J Immunol 2000; 165(2):618–22.

[74] Goldman SR, Tu Y, Goldberg MB. Differential regulation by magnesium of the two MsbB paralogs of *Shigella flexneri*. J Bacteriol 2008;190(10):3526–37.